Selectivity analysis of an incoherent grating imaged in a photorefractive crystal

Myrian Tebaldi[1,2], Gustavo Forte[1,3] , Nestor Bolognini[1,2,3] and Maria del Carmen Lasprilla A. [4]

[1] Centro de Investigaciones Ópticas, CIOp (CONICET La Plata – CIC - UNLP), P.O. Box 3, 1897, Gonnet, La Plata, Argentina

[2]UIDET OPTIMO, Departamento de Ciencias Básicas, Facultad de Ingeniería, Universidad Nacional de La Plata, Argentina

[3]Departamento de Física, Facultad de Ciencias Exactas, Universidad Nacional de La Plata, Argentina

[4]Escuela de Física, UIS, Bucaramanga, Colombia

In this work, the diffraction efficiency of a volume phase grating incoherently stored in a photorefractive BSO crystal is theoretically and experimentally analyzed. The results confirm the theoretical proposal based on the coupled wave theory adopting a new grating depth parameter associated to the write-in incoherent optical system. The selectivity behavior is governed by the exit pupil diameter of the imaging recording system that controls the depth of the tridimensional image distribution along the propagation direction. Two incoherent gratings are multiplexed in a single crystal and reconstructed without cross-talk.

Keywords: volume grating, incoherent optical system, BSO crystal

1. Introduction

Holographic data storage is usually employed in optical systems [1 - 4]. The holograms are classified in thin and volume depending on its diffraction behavior. It is well known that a thin phase grating holographically produced exhibits Raman-Nath behavior and a thick phase grating presents Bragg behavior in the diffraction process [5, 6]. In the Raman-Nath regime several diffracted waves are

produced. We refer by quasi-Bragg diffraction to the intermediate regime where the volume grating assumption is no longer fully valid. This is the transition between the Raman-Nath and the Bragg regimes. In this case, the Bragg condition relaxes and there may be significant scattering into other than the desired orders.

In photorefractive materials like a sillenite BSO crystal, volume phase holograms are stored by the interference of two coherent beams inside the crystal [7]. The volume nature of the register becomes noticeable when the diffraction of the read-out beam is observed. A rigorous analysis of the volume holographic gratings diffraction efficiency involves the coupled-wave theory [8]. This theory predicts a non-zero diffraction efficiency when a plane wave is incident on a grating with an angle different from that determined by the Bragg condition. Several experimental and theoretical study of the angular selectivity in volume recording media are presented in the literature [9,10].

The gratings generated by the interference of two beams are holographic procedures. In previous work it is demonstrated that the interference of two speckle patterns behave as predicted by the coupled wave theory [11-13]. On the other hand, in the photorefractive incoherent to coherent optical converter (PICOC) [14], an incoherent image is focused in the volume of a photorefractive crystal in addition to the coherent interfering beams, producing an additional spatial modulation of the charge distribution stored. This incoherent modulation is transferred onto the coherent beam by reconstructing the holographic grating. It should be pointed out that all the previous cases involve interference patterns.

In our work, an input grating is incoherently imaged resulting in a tridimensional intensity distribution controlled by the exit pupil of the optical system. Note that in this case no interference procedure is involved. This non-holographic grating is stored on a birefringence modulation basis by using a thick photorefractive BSO crystal. The aim of our proposal is to characterize the light intensity diffracted by this non-conventional volume phase grating when a coherent beam impinges to the crystal. In our analysis, it is stablished that the input grating frequency, the crystal thickness and the tridimensional intensity distribution govern the angular selectivity behavior.

As it is well known holographic gratings should exhibit Bragg behavior. Then, several gratings can be stored in a crystal volume without cross talk. There are different methods to record several holograms with non-coincident grating wave vectors; for instance, by changing the wave vectors direction and modulus which depends on the writing wavelength and the angle between interfering beams [15,16]. Finally, we verified experimentally the possibility to multiplex without cross-talk two incoherently registered gratings in a single BSO crystal.

2. Experimental arrangement and theoretical background

In Ref. [18], we analyze the light intensity distribution generated by an incoherently illuminated planar amplitude grating. The intensity distribution at the image plane and in its neighborhood, are described by the optical transfer function (OTF) corresponding to an incoherent imaging system [17,18]. Then, this distribution spreads in a finite volume region. In particular for a fixed input grating frequency, the tridimensional image distribution is governed by the imaging system exit pupil diameter. In fact, a decreasing exit pupil diameter enlarges the region in which the projected image grating exists. In this reference, the theoretical simulation is compared with the experimental data of the 3D intensity distribution on the basis on a pure incoherent source. A good coincidence enabled us to disregard the possible effect of a partial coherence propagation.

In order to highlight the tridimensional characteristics of the mentioned image grating a volume recording medium must be utilized. A photorefractive BSO crystal sample is used for the detailed purpose.

Let us consider the experimental scheme depicted in Figure 1. In the write-in step, a Ronchi grating G is illuminated with an incoherent white light source by the condenser lens L_1. An image of the incoherently illuminated grating G with unitary magnification is formed into the BSO crystal sample by a lens L_2 (focal length f = 50 mm). Lens L_2 has an iris diaphragm of variable aperture diameter D attached in front of it. The input grating G has frequencies between 10 lines/mm to 30 lines/mm. The BSO crystal has strong photoconductivity in the green region of the spectrum and an interference green filter (λ_w = 530 nm ± 3 nm) is used in the write-in step. The BSO crystal is cut normally to the $\langle \bar{1}10 \rangle$ crystallographic direction. The crystals used in the experiment were provided from Fujian Castech Crystals, Inc**.** and are rectangular parallelepipeds cut along the (110), $(1\bar{1}\,0)$ and (001) planes and polished better than λ/4 at the $(1\bar{1}\,0)$ faces. The physical dimensions of the crystals are *Lx*=10 mm, *Ly=10* mm and different values of L_z. An external electric field is applied to the crystal (110) planes.

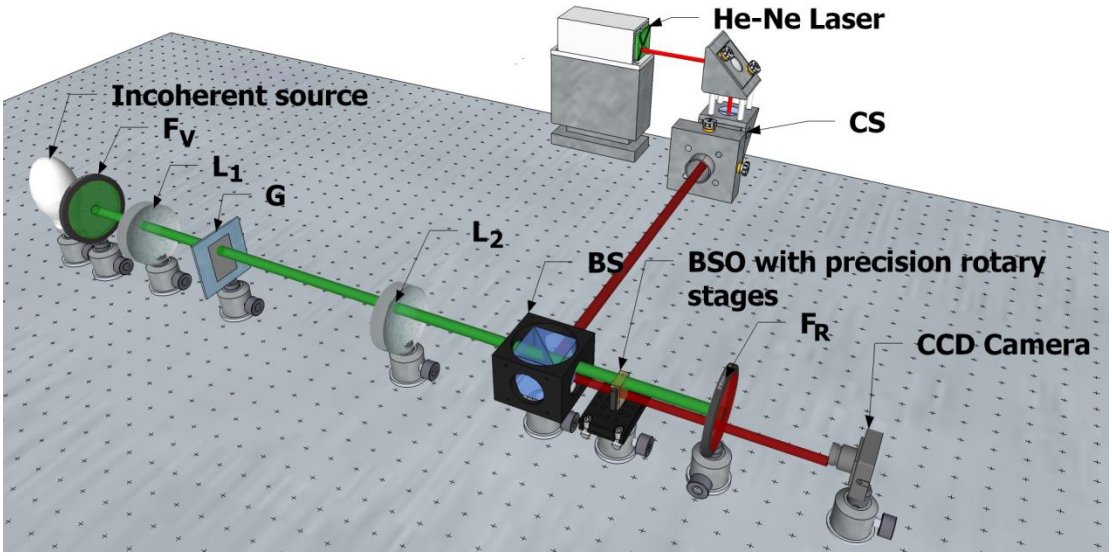

Figure 1 Experimental scheme (F_V: green interference filter (λ_W=530 ± 3 nm); L_1 and L_2: lenses; G: grating; BS: beam splitter; F_R: red interference filter (λ_R= 632,8 ± 3 nm); CS: spatial filter and collimator system).

As a first step, it is necessary to analyze the tridimensional intensity distribution of our incoherent imaging system. The grating G is imaged by using a quasi-monochromatic white light source. In Figure 2 the tridimensional intensity distribution generated by the system is simulated by using the respective OTF function corresponding to a region of +/- 5mm with respect to the image plane. The results correspond to different values of the exit pupil diameter D. It should be observed the dependence between the spread of the light intensity distribution and the mentioned parameter D. It is evident that a reduction in the pupil diameter highly increases the depth of the light intensity distribution.

This distribution is registered in a volume medium by employing a photorefractive crystal. This medium allows to store the mentioned whole distribution including the miss-focused region. Concerning the grating frequency in an incoherent recording, it should be considered the effect of the existing frequencies near the cut off value of the incoherent system. Taking into account that those frequencies contribute with low intensity, the incoherent recording do not lead to the generation of a measurable index grating perturbation via the photorefractive effect. The actual cut off frequency which can be mapped as phase grating is much lower than the incoherent optical system cut off frequency. Finally, by considering the geometrical effect in our experimental arrangement a grating with a maximum of 30 lines/mm is utilized.

In Figure 2, a 10 mm depth region of the tridimensional intensity distribution is displayed. Note that, when a crystal with the same10 mm thickness is considered, by observing the tridimensional plot

of Figure 2 it is seems that only a limited region in the crystal generates a measurable index phase grating. The mentioned region corresponds to the main lobes. In summary, a fraction of the volume sensitive medium generates a significant index phase grating.

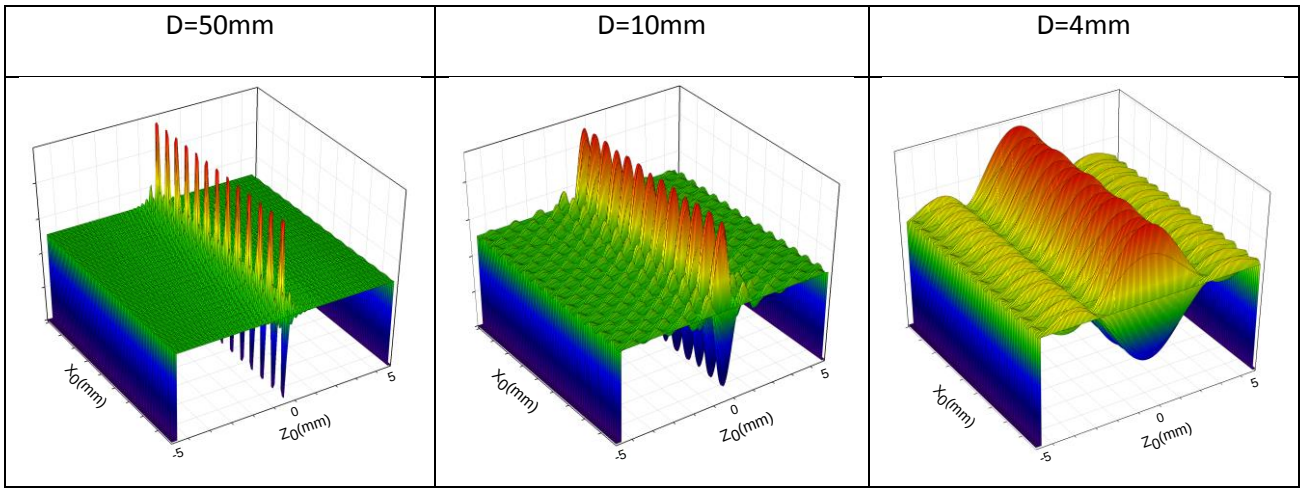

Figure 2. 3D incoherent intensity distribution corresponding to a 30 lines/mm grating for different exit pupil diameters *D*.

The incoherent intensity distribution projected into the crystal is mapped as an index refractive perturbation Δn via the photorefractive effect. The spatial pattern of the input grating creates a phase grating in the photorefractive material by modulating the index of refraction n so that $n = n_0 + \Delta n$, where n_0 is the bulk refractive index. In the photorefractive process, the amplitude of the index grating modulation depends on the amplitude of the space-charge field which is controlled in our experimental condition essentially by the external electric field. Note that the low spatial frequency involved in the incoherent register implies a negligible value of the diffusion field and thereby the external applied field controls the strength of the index grating perturbation. There is no phase shift between the input intensity distribution and the photorefractive volume grating. A model to describe the volume photorefractive phase grating generation is outlined in Ref. [19].

Note that, the photorefractive effect is based on intensity gradient detection and no matter the degree of coherence of the intensity distribution that the crystal receives. The selection of the incoherent source in our experiment is based exclusively on the better signal to noise ratio presented in this situation.

The volume nature of the periodic stored information becomes noticeable when the diffraction of the read-out beam is detected. The phenomenon of light diffraction by periodic phase gratings has been extensively analyzed by several authors. The coupled wave theory for the transmission geometry predicts a non-zero diffraction efficiency when a plane wave is incident on a finite grating at an angle different from that determined by the Bragg condition [8]. The theoretical treatment for finite thickness holographic grating considers an additional wave vector, called off-Bragg vector. In accordance with this model the diffraction efficiency of the index grating gives:

$$\eta = \frac{\kappa^2}{\kappa^2 + \left(\frac{\xi}{2}\right)^2} \sin^2\left(L\sqrt{\kappa^2 + \left(\frac{\xi}{2}\right)^2}\right) \tag{1}$$

where L is the crystal thickness, $\xi = \left|\vec{\Omega}\right| \left(\frac{\cos(\theta)}{\sqrt{n_0^2 - \sin^2(\theta)}}\right) \Delta\theta$ is the off-Bragg parameter, $\left|\vec{\Omega}\right|$ is the modulus of the index grating-vector, θ is the external Bragg angle in the read-out step ($\theta = \frac{\lambda_R}{\lambda_W}\theta_0$ where θ_0 is the write-in angle, λ_W and λ_R is the write-in and the read-out wavelength, respectively), $\Delta\theta$ is the off-Bragg read-out angle, $\kappa = \frac{\pi\, n_0\, \Delta n}{\lambda_R \sqrt{n_0^2 - \sin^2(\theta)}}$ is the coupling coefficient and Δn is the index grating modulation depth. The general expression for index modulation Δn is:

$$\Delta n = \frac{n_0^3\, r_{41}\, m}{2} \left[\frac{E_D^2 + \left(\vec{E}_a \cdot \vec{\Omega}\right)^2}{\left(1 + \frac{E_D}{E_q}\right)^2 + \frac{\left(\vec{E}_a \cdot \vec{\Omega}\right)^2}{E_q^2}}\right]^{1/2} \tag{2}$$

where r_{41} is electro optic coefficient, $m = 2\dfrac{\sqrt{I_1 \cdot I_2}}{I_1 + I_2}$ is the modulation of the interfering beams (I_1 and I_2 are the intensity of the write-in interfering beams), E_D is the diffusion field, E_q is the maximum space charge field, E_a is the external applied field and $\hat{\Omega}$ is the index grating versor. For the grating frequency range considered, the diffusion field can be disregarded and $E_a << E_q$, then the expression results,

$$\Delta n = \frac{n_0^3\, r_{41}\, m}{2}\left(\vec{E}_a \cdot \hat{\Omega}\right) \tag{3}$$

In our experiments the value of the BSO electro-optic coefficient is r_{41}=3.5 pm/V and the refractive index without induced field is n_0= 2.54.

In Ref. [20], the information illuminated with an incoherent source is stored in the crystal. In this context, the volume nature of the stored information was not considered. However, we have envisaged the volume influence [17-18] when analyzing the Talbot and Lau fringes visibility. The purpose of our work is to confirm the previous observation, through the evaluation of the diffraction efficiency of the 3D periodic distribution imaged in the crystal.

In a holographic recording, the index modulation represents the index gradient of the diffraction planes built by the photorefractive process. On the other hand, the register of the incoherent grating G through the photorefractive effect provides the mentioned index gradient. Once the phase grating is generated, it is evaluated by using a low power linearly polarized He-Ne beam of wavelength λ_R= 632,8 nm impinging onto the crystal. This wavelength is outside of the crystal spectral sensitivity, therefore avoiding information degradation.

In the following section, we evaluate the angular selectivity response associated to the stored incoherent grating. The BSO crystal sample is mounted in a precision rotatory stage providing thereby a change in the angle between the read-out light direction and the crystal normal direction of the input

crystal plane. As far as the read-out beam direction is rotated the diffraction efficiency changes and the angular selectivity can be measured.

3. Stored grating evaluation

In the following, the diffraction efficiency of the incoherent input grating stored in the crystal is evaluated. Note that in the conventional coupled wave theory the parameter L which controls the available diffraction is the crystal thickness (see Eq. (1)). In our proposal, it is necessary to define an effective thickness L_{effec} where the phase grating is significantly strong so that a noticeable diffraction is expected in the read-out step. Then, in the coupled wave theory the parameter L must be defined as

$$L = \begin{cases} L_{effec} & if \quad L_{effec} < L_Z \\ L_Z & \text{other cases} \end{cases} \tag{4}$$

where L_{effec} corresponds to the depth of the main lobe of the 3D incoherent image distribution as was analyzed in the previous section.

The use of this new parameter in the coupled wave theory is verified through a proper evaluation of the diffraction efficiency. This fact is experimentally confirmed in Figure 3, where the diffraction efficiency for different crystal thicknesses is depicted. There, defined diffraction spots are observed which are measured in the read-out step (see Figure 3). Note that in this case the grating frequency and the imaging system pupil aperture D are maintained fixed. In Figure 3, the grating frequency and the imaging system pupil diameter D are maintained. The parameter L_{effec} is the same in all cases and approximately equal to 1 mm. Note that the different crystal thicknesses employed are larger than L_{effec} in all cases, then the parameter L is the L_{effec} in all results. In summary, the same selectivity behavior is observed confirming our original assertion.

As analyzed in the previous section, the spread of the input light intensity distribution changes with imaging system exit pupil diameter D. A reduction in the pupil diameter highly increases the depth of

the main lobe of the tridimensional distribution. In order to confirm this fact, we evaluate the normalized intensity of the diffraction efficiency of the incoherently stored grating in terms of the off-Bragg angle read-out for different values of the diameter D. Figure 4 shows experimental results and theoretical curves. All results correspond to a grating with a 30 lines/mm frequency and a BSO crystal with L_Z=10 mm and E_a = 6 kV/cm. Then, $L_Z > L_{effec}$ and in the theoretical calculation the parameter L must be replaced by the L_{effec} which depends on how distributed is the incident intensity in the crystal (see Figure 2). Figure 4 shows that the value of the on-Bragg diffraction efficiency is greater in the case of D = 4mm in comparison with D = 10 mm and D = 50 mm. Also, a sharper angular selectivity is observed for the minimum pupil aperture diameter D. A good agreement between the theoretical calculated and the measured diffraction efficiency can be observed. It should be emphasizing that this result represents the demonstration of the volume built grating under an incoherent illumination which effectively produces directional diffraction in the read-out step.

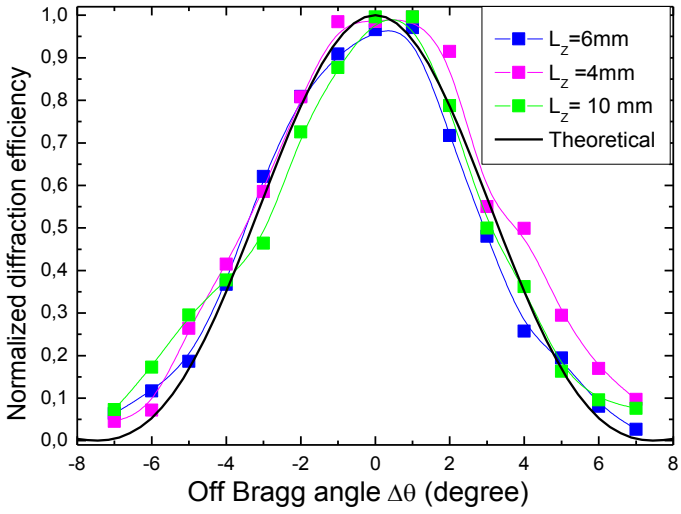

Figure 3 Normalized diffraction efficiency corresponding to a 20 lines/mm grating, the exit pupil diameter of the write-in optical system is D=14 mm, BSO crystal with E_a = 6 kV/cm and different thicknesses L_Z. The continuous black lines correspond to the theoretical curve calculated with the experimental parameter

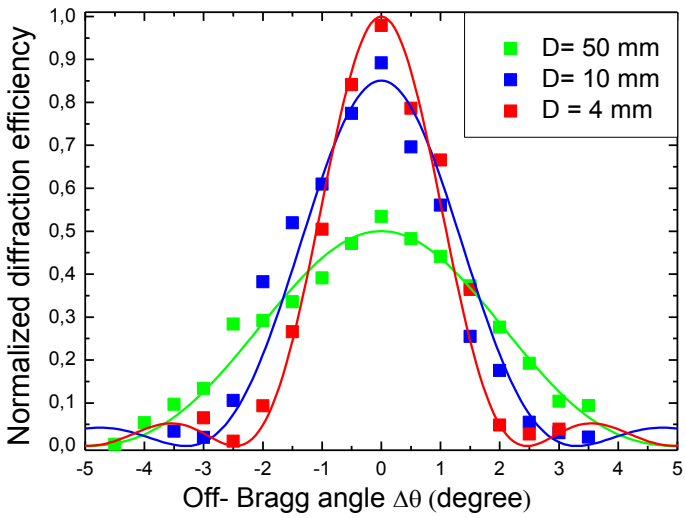

Figure 4 Normalized diffraction efficiency corresponding to a 30 lines/mm grating stored in a BSO crystal with E_a = 6 kV/cm, L_Z = 10 mm and for different exit pupil apertures. The continuous lines correspond to the respective theoretical calculation results.

As mentioned in the introduction a thin phase grating exhibits Raman-Nath behavior and a volume phase grating presents Bragg behavior in the diffraction process. An interesting parameter to measure the degree of the volume behavior is defined as,

$$Q = \frac{2\pi\,\lambda_W\,L}{n_0\Lambda^2} \tag{5}$$

where λ_W is the wavelength, L is the thickness of the volume phase grating in the propagation direction, Λ is the grating spacing. The gratings with values of $Q < 1$ operate in general under Raman-Nath regime and several diffracted waves are produced. Gratings with $Q \geq 10$ operates in Bragg regime. However, it is observed Raman-Nath for very large values of Q. In our proposal, the parameter L is given by expression (4) where L must be replaced by the L_{effec} if $L_{effec} < L_Z$. Therefore, this change should be extended to the mentioned Q parameter. Then,

$$Q = \frac{2\pi\,\lambda_W\,L_{effec}(\mathrm{D})f^2}{n_0} \qquad \text{if} \qquad L_{effec} < L_Z \tag{6}$$

Concerning the Q parameter associated to the results of Figure 4, as far as the pupil diameter decreases the Q value increases accordingly. The Q values are: 1.12 for D = 50 mm, 7 for D = 10 mm and 25.58 for D = 4 mm.. As can be deduced from the two first Q values calculated above our results fits in the mentioned quasi-Bragg diffraction regime where the volume grating assumption is no longer fully valid. The last value (Q >10 for D = 4 mm) demonstrates the possibility to generate volume phase grating by employing an incoherent source recording.

Then, we evaluate the diffraction efficiency with gratings of different frequencies. To this end, we first analyze the L_{effec} behavior derived from the OTF. Figure 5 shows the L_{effec} values obtained from the tridimensional distribution in terms of the exit pupil diameter of the write-in optical system. It clearly shows that lower pupil aperture diameters produce a significative change in the parameter L_{effec} of the phase grating when different frequencies for the input grating are utilized. On the other side, for values of the pupil aperture diameter D > 30 mm, the influence of the grating frequencies are negligible as observed in Figure 5.

In Figure 6, the diffraction efficiency in terms of the off-Bragg angle $\Delta\theta$ for different grating frequencies is displayed. In fact, the diffraction lobes of the intensity distribution change also as the input grating frequency is modified. In particular the main lobes change inversely with their width as the grating frequency changes. For example, in the case of D=18 mm a non-significant change in L_{effec} is produced.

Two effects must be considered simultaneously in the evaluation of the parameter Q. First, the parameter L_{effec} is higher for the minimum frequency of 10 lines/mm. Second, the parameter Q is directly proportional to the effective thickness and to the square of the grating spatial frequency. As mentioned a frequency increase implies a L_{effec} parameter decrease. For gratings with frequencies of 10 lines/mm, 20 lines/mm and 30 lines/mm, the Q parameter results: 1.5, 3.3 and 5.2 respectively. Taking into account the dependence on the frequency, the parameter Q should increase nine times from 10

lines/mm to 30 lines/mm. However, it has changed three times due to the L_{effec} increase. In summary, the parameter Q increases with the grating frequency. Then, the angular selectivity becomes more evident for a 30 lines/mm as is observed in Figure 6.

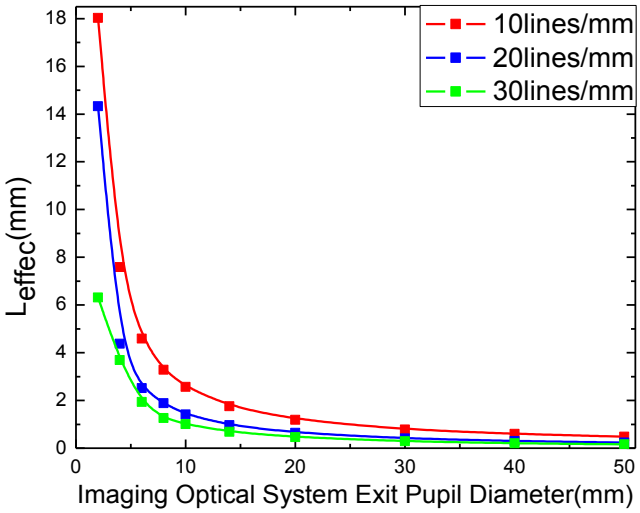

Figure 5: Theoretical L_{effec} values obtained from the OTF function in term of the exit pupil diameter of the write-in optical system

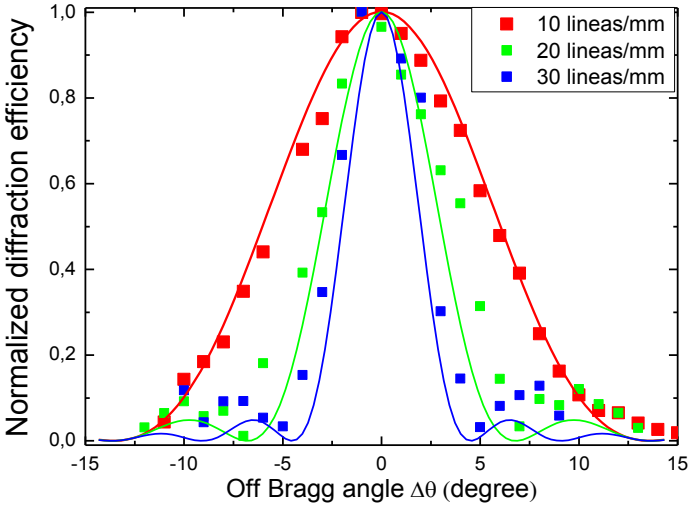

Figure 6. Normalized diffraction efficiency for different grating frequencies and for a BSO crystal with E_a = 6 kV/cm, L_Z=3 mm and an exit pupil aperture diameter D=18 mm.

4. Multiplexing implementation

We now propose to multiplex incoherently stored data in a single photorefractive BSO crystal. In our case, the sample rotation is an easy method to implement the multiplexing. The multiplexing is achieved when the crystal is rotated around an axis perpendicular to the plane of incidence between the consecutive recordings of two gratings of the same frequency. In this case, the **Ω** vectors of the data differ mainly in their directions, although slightly in their modules. Then, this orientation multiplexing is characterized by different gratings vector **Ω**. The readout address of each datum is given by the orientation of the write-in beam relative to the sample normal. As analyzed in the previous section, the reconstruction of the stored data occupies an angular spread which must be considered in order to avoid cross talk. By Eqs. (1) and (4) we can observe that the angular spread (Bragg peak angular width) occupied by one datum is smaller for a smaller pupil aperture diameter.

A He-Ne laser beam is used to measure the variation of the diffraction efficiency while the sample is rotated around the Bragg angle associated to each multiplexed datum. Experimental evaluation of the diffraction efficiency demonstrates the possibility to multiplex by using the incoherent recording system (see Figure 7). As it can be seen in this figure, each register is angularly resolved without cross-talk.

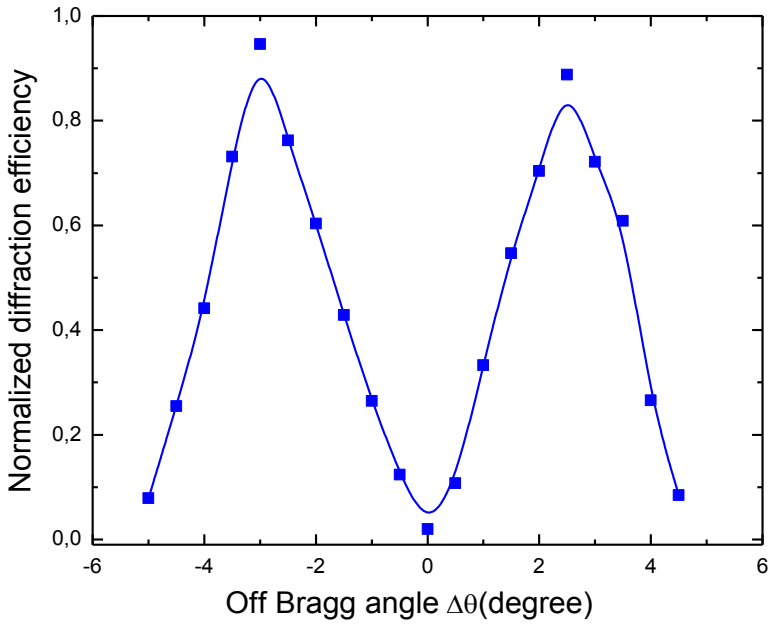

Figure 7. Angular dependence of the diffracted intensity produced by two angular multiplexed volume data, stored for angular crystal orientation of -3 ° and 3° with respect to the crystal incidence plane perpendicular.

5. Conclusion

The key point of this work is to demonstrate that an incoherent optical system can be used to generate a volume phase grating susceptible to replicate the selectivity behavior presented in holographically generated gratings.

In particular, we experimentally verified that an optical incoherent recording can be arranged to obtain a volume phase grating in a photorefractive crystal and the associated spatial selectivity is measured through the diffraction process. It must be emphasized that the diffraction spots are observed and measured in the read-out step in the proposed incoherent to coherent optical converter.

The image intensity distribution generated in the photorefractive crystal is controlled by the optical system exit pupil. This fact implies that we need to consider a new effective length parameter to be taken into account when modeling. This parameter is not necessary to be introduced in the holographic gratings, because the useful grating depth coincides with the thickness of the recording medium itself.

Our proposal is verified by using a photorefractive crystal as recording medium. However, the results are more general and they could be probed in another volume support.

As it is mentioned above, in our case none interference procedure is involved. Due to the nature of our proposal is constrained to low spatial frequencies (lower that 30 lines/ mm) which limits the value of the diffraction efficiency. However, lower stability is required. In addition, our method has a good signal to noise ratio which characterize incoherent optical systems.

Finally, the application of this incoherent optical converter allows implementing information multiplexing as usual in holographic volume media.

Acknowledgments

This research was performed under the grants: CONICET No. 0849/16 and 0549/12 (Argentina) and Facultad Ingeniería, Universidad Nacional de La Plata No. 11/I215 (Argentina).

References

[1] P. Hariharan, Optical Holography Principles, Techniques and Applications, Cambridge University Press, 1996.

[2] L. Solymar, Volume Holography and Volume Gratings, Academic Press, London, 1981.

[3] R. R. A. Syms, Practical Volume Holography, Oxford Science Publications, 1990.

[4] J. F. Barrera, R. Henao, M. Tebaldi, R. Torroba, N. Bolognini, Code retrieval via undercover multiplexing, Optik, 119 (2008) 139-142.

[5] M. G. Moharam, L. Young**,** Criterion for Bragg and Raman-Nath diffraction regimes, Appl. Opt. 17 (1978) 1757-1759.

[6] M. G. Moharam, T. K. Gaylord, R. Magnusson, Criteria for Raman-Nath regime diffraction by phase gratings, Opt. Commun. 32 (1980) 19-23.

[7] C. Gu, Y. Xu, Y. Liu, J.J Pan, F. Zhou, H. He, Applications of photorefractive materials in information storage, processing and communication, Optical Materials 23 (2003) 219-227.

[8] H. Kogelnik, Coupled wave theory for thick hologram gratings, Bell Syst. Tech. J. 48 (1969) 2909-2947.

[9] J. M. Heaton, P. A. Mills, E. G. S. Paige, L. Solymar, T. Wilson, Diffraction efficiency and angular selectivity of volume phase holograms recorded in photorefractive materials, Optica Acta 31 (1984) 885-901.

[10] J. V. Alvarez-Bravo, N. Bolognini, L. Arizmendi, Experimental study of the angular selectivity of volume phase holograms stored in LiNbO3, Appl. Phys. B, 62 (1996) 159-164.

[11] M. Tebaldi, A. Lencina, N. Bolognini, Analysis and applications of the speckle patterns registered in a photorefractive BTO crystal, opt. Commun. 202 (2002) 257-270.

[12] M. L. Molina Prado, M. C. Lasprilla, M. Tebaldi, N. Bolognini, Slope detection method by modulated speckle patterns, optik.122 (2011) 228 – 234.

[13] M. Tebaldi, L. Angel Toro, M. C. Lasprilla, N. Bolognini, Image multiplexing by speckle in a BSO crystal Opt. Commun. 155 (4), 342-350 (1998).

[14] J. W. Yu, D. Psaltis, A. Marrakchi, A. R. Tanguay, R. V. Johnson, The photorefractive incoherent-to-coherent optical converter, in P. Gunter and J. P. Huignard (Eds), Photorefractive Materials and Their Applications II, Springer Verlag, 1989, 275-324.

[15] F. H. Mok, Angle-multiplexed storage of 5000 holograms in lithium niobate, Opt. Lett. 18 (1993) 915-917.

[16] M. Tebaldi, S. Horrillo, E. Pérez-Cabré, M.S. Millán, D. Amaya, R. Torroba, N. Bolognini, Experimental color encryption in a joint transform correlator architecture, Journal of Physics: Conference Series 274 (2011) 012054.

[17] G. Forte, A. Lencina, M Tebaldi, N Bolognini, Talbot effect by a photorefractive volume phase grating, Appl. Opt. 51 (2012) 479-485.

[18] G. Forte, M. Tebaldi, N. Bolognini, Study of Lau fringes generated by a photorefractive volume grating, Opt. Commun. 396 (2017) 110-115.

[19] J. P. Huignard and P. Gunter, Optical processing using wave mixing in photorefractive crystals, in P. Gunter and J. P. Huignard (Eds), Photorefractive Materials and Their Applications II, Springer Verlag, 1989, 205-273.

[20] M. C. Lasprilla A., A. Agra Amorim, M. Tebaldi, N. Bolognini, Self-imaging through incoherent to coherent conversion Opt. Eng. 35 (1996) 1440-1445.